Supplementary Information

Calculations

The whisker was modeled as a straight cantilever beam rotating against a rigid, motionless object. This model is justified because rat whiskers exert miniscule contact forces and rat whisking movements are very rapid. The derivation that follows could be done in terms of force instead of moment, and/or translation instead of rotation.

The Euler-Bernoulli equation relates the curvature $\kappa(x)$ at every point along the beam to the moment $M(x)$ at that point[1, 2, 3]. For a point load F at a distance d yielding a small deflection $y(d)$, $M(x) = F(d - x)$ and the equation can be linearized:

$$\kappa(x) \approx \frac{\mathrm{d}^2 y}{\mathrm{d}x^2} \approx \frac{F(d-x)}{EI}. \tag{S1}$$

For a cone, the whisker radius will vary linearly along the length, giving an area moment of inertia of

$$I = I_{base}\left(1 - \frac{x}{L}\right)^4 \tag{S2}$$

where $I_{base} = \pi / 4 \cdot r_{base}^{\ 4}$ and r_{base} is the whisker radius at its base. Inserting Eqn. S2 into Eqn. S1, integrating twice and solving for the deflection at d yields

$$y(d) = \frac{FLd^3}{3EI_{base}(L-d)}. \tag{S3}$$

Substituting $M = d \times F$ and $\theta = y(d)/d$,

$$M = C\theta\left(\frac{1}{d} - \frac{1}{L}\right) \tag{S4}$$

where $C = 3EI_{base}$. Taking the time derivative on both sides and solving for d yields

$$d = \frac{C\dot{\theta}L}{C\dot{\theta} + \dot{M}L}. \tag{S5}$$

The time derivative ensures biological plausibility. In robotic or engineered systems d can be computed directly using θ and M. In contrast, animal nervous systems are generally poor at judging absolute values, but quite good at judging rates of change in values. This general principle is true across visual, auditory, tactile and olfactory systems.

For a cylinder (e.g., the robotic whiskers), whisker radius is constant along the length, allowing immediate integration of Eqn. S1. Solving for the deflection and substituting $M = d \times F$ and $\theta = y(d)/d$, we find

$$M = C\frac{\theta}{d}. \tag{S6}$$

Solving for *d*,

$$d = C\frac{\theta}{M}. \tag{S7}$$

Equation S7 shows that a motor rotating a cylindrical beam against a point object will experience a torque proportional to the amount it is rotated (for small values of θ). In other words, the beam acts as a torsional spring, with an effective spring constant inversely proportional to object distance *d*. This result was also found by Kaneko *et al.*[1] but is included here for completeness.

To account for lateral (up-down) slip of the whisker, Eqn. S7 must be multiplied by a factor related to the slope of the surface. If we assume that the surface being contacted is flat and frictionless, Eqn. S7 becomes

$$d = C\frac{\theta}{|M|}\cdot\cos\beta \tag{S8}$$

where $|M| = \sqrt{M_x^2 + M_y^2}$, M_x is the component of the moment in the direction of the axis of rotation, M_y is the component of the moment in the lateral plane and $\beta = \tan^{-1}(M_y / M_x)$. Note that although most surfaces encountered (including our sculpted head) will have both non-zero curvature and friction, the two-dimensional modification of Eqn. S8 helps to improve distance extraction accuracy.

It is informative to note that Eqns. S4 and S6 can both be rewritten in a general form relating $\dot{M}$ to $\dot{\theta}$ (or *M* to θ) through a stiffness function *k(d)*:

$$\dot{M} = k(d)\dot{\theta} \tag{S9}$$

where *k*(*d*) is a monotonically decreasing function that depends on the geometry and elastic modulus of the whisker. The implication is that object distance *d* can always be uniquely inferred from measurement of $\dot{M}$ for any given the whisking velocity $\dot{\theta}$. The

shape of the curve defined by Eqn. S9 can be analytically derived as shown above, or learned through interaction with the environment.

Alternative Methods for the Estimation of Radial Contact Distance

There are at least three alternative methods of computing radial contact distance using sensors only at the whisker base. One seemingly-straightforward approach would be to measure force and moment simultaneously[2] and then calculate the distance d from the well-known equation $d = M/F$. In practice, however, the simultaneous, independent measurement of force and moment is extremely difficult. Multi-axis sensors that can provide independent measurements of moment and force are prohibitively bulky and expensive for small-scale whisker arrays, and it is highly unlikely that biological sensors in the follicle can measure the two quantities independently.

Another possible approach is to measure the vibrations associated with collision and correlate them with object distance[4]. However, several lines of evidence strongly suggest that bending moment is a critical variable for the rat, and vibrations alone are unlikely to permit the rat to determine radial distance. (1) Previous work has shown that whiskers are quite damped, limiting the amplitude and duration of any signals transmitted to the base. This means that if there is any noise in the signal, it will be difficult to obtain an accurate estimate of object distance. In contrast, if whisking velocity is constant (a good approximation for the real rat), $\dot{M}$ will be constant for a large fraction of the whisk. This means the rat has a comparatively long time to take an average measurement of $\dot{M}$ and $\dot{\theta}$, and thus obtain a robust estimate for object distance. (2) Vibrations due to object contact would likely overlap with those caused by object texture, thus generating a signal that contains ambiguous information about texture and distance.

A third method, less suitable for robotic applications, incorporates the dynamics of the whisker-follicle complex and the surrounding sling muscle. Movement of the entire follicle-whisker complex could be obstructed in a distance-dependent manner, or sling-muscle force could likewise vary with radial contact distance. Cells responsive to these phenomena could thus encode contact distance[5]. This mechanism is likely to work in conjunction with the moment produced by the whisker inside the follicle as described in the present manuscript.

A recent study has confirmed that some primary sensory neurons in the trigeminal ganglion spike as would be expected if they were primarily responding to the rate of change in bending moment at the whisker base[5]. In summary, we postulate that the time derivative of moment (or curvature, which is proportional to moment) is the primary cue used by the rat to estimate object distance. As nervous systems are renowned for exploiting all available information, vibrations may secondarily contribute to the distance estimation.

Numerical Simulation Methods

Although Eqn. S5 assumes that the whisker is straight, rat whiskers actually have significant inherent curvature. Therefore, numerical simulation was used to confirm that this inherent curvature has negligible effect on the accuracy of Eqn. S5. Because the whisker diameter is much less than its radius of curvature, classical elasticity theory can be used[3]. The numerical routine is based on the following premise: for a given force $\overline{F}$ acting at a given arc length S from the base of a beam defined by coordinates (x, y), the resulting beam shape can be found through repeated application of

$$\mathrm{d}\kappa_i = \frac{\bar{r}_i \times \overline{F}}{EI_i} \tag{S10}$$

where $\mathrm{d}\kappa_i$ is the change in curvature at node i, $\bar{r}_i$ is the vector connecting node i to S, and I_i is the second moment of inertia at node i. Assuming no friction, $\overline{F}$ will always act normal to the arc length. As shown in Fig. S1, a node 0 is placed (through linear interpolation) at S. Equation S10 is then applied node-by-node towards the beam base to compute the resulting shape. Matlab's 'fminsearch' function was used to find the unique $\overline{F}$ and S that caused the beam to intersect a desired deflection point (a, b). To create Fig. S2, we used this numerical routine on increasingly curved beams (whiskers). Whisker curvature is normalized by whisker arc length, and radial distance units d are normalized by whisker base-to-tip length L. The beams were assumed to be circular arc segments with central angles of $\pi/4$, $\pi/2$ and π (central angle is equivalent to normalized curvature for beams with constant curvature). A normalized curvature of $\pi/4$ is typical along whiskers, $\pi/2$ exceeds the maximum curvature along most whiskers, and π is well above

the curvature seen in rat whiskers. The theoretical finding that curvature will have a negligible effect on the bending of the whisker was then verified experimentally (see next section).

Experimental Characterization of Rat Whiskers

Linear elasticity theory is well-established, but for Eqn. S5 to accurately describe the deformations of a real rat whisker several assumptions must hold true:

1. The whisker material can be modeled as homogeneous and the elastic modulus is thus constant along the length.
2. The whisker tapers linearly from base to tip.
3. The inherent curvature of the whisker has a negligible effect (consistent with the numerical result).

Equation S5 was verified experimentally as a real (plucked) rat whisker was smoothly rotated against a slender peg placed at increasing radial distances. The whisker was 45 mm in base-to-tip length, and was glued with cyanoacrylate to a strain gage to measure moment at the whisker base. The strain gage was then attached to the shaft of an AC servo motor, such that the whisker base was at the center of rotation (Fig. S3). Because the stiffness of the strain gage was significantly greater than that of the whisker, it bent negligibly compared to the whisker. This meant that the whisker base always stayed fixed at the center of rotation. The strain gage was incorporated into a Wheatstone bridge and analog voltages were filtered at 500 Hz and subsequently sampled at 2 kHz. All data analysis was performed in MATLAB v7.0.

Strain gage voltage was calibrated to moment only at a single radial distance. First, a 30 mg calibration weight was hung from the whisker 1 cm from the base and the deflection photographed with a high resolution digital camera. The photograph provided a single deflection/moment ratio. Linearity was confirmed with a series of smaller calibration weights. Second, the weight was removed, and the whisker was slowly rotated against a slender peg (1.6 mm diameter) again placed at a radial distance of 1 cm. Ten whisks were performed at 45 deg/sec through an amplitude of 22.5˚. Signals were filtered with a zero-phase forward digital filter (period = 1/3 second) and averaged over the ten whisks. This data set served to calibrate between strain gage voltage and deflection, and

compensated for nonlinearities in the strain gage voltage for small values of moment. Third, we scaled the voltage/deflection curve by the deflection/moment ratio, yielding a moment vs. voltage calibration curve for all experimental data.

The data shown in Fig. S4 were taken with the peg placed at distances varying from 5 mm to 35 mm, in 2.5 mm increments. Ten whisks were performed at 45 deg/sec through an amplitude of 22.5˚. Signals were filtered and averaged over the ten whisks. Figure S4 (blue circles) shows estimates of radial object distance (d_{est}) calculated from Eqn. S5 with $C = 0.298$ μN·m^2 obtained by a least squares fit. The error in the estimate grows towards the tip of the whisker, as sensor noise (error in $\dot{M}$) has an increasing effect on the calculation of d_{est} (Fig. S4, red triangles).

A digital scan of the whisker base was taken with a microscope at 20X magnification, and the diameter was found to be 155 μm, yielding a second moment of inertia $I = 2.83\times10^{-17}$ m^4. For the fitted value of $C = 0.298$ μN·m^2, this yields an elastic modulus E of 3.50 GPa, which is well within the range of previously established values[6,7,8].

The advantage of having an analytic relationship as expressed in Eqn. S5 is that it allows neuroscientists to estimate M and its time-derivative at the base of a whisker in the intact animal, based on known or easily measurable quantities: θ, E, L and r_{base}. This tool will allow the electrophysiological responses of whisker-related neurons to be correlated with the mechanical state of the whisker.

Feature Extraction Methods

Calibration between voltage and moment for the artificial whisker array was performed by sweeping each whisker five times against a peg placed at a single distance of 2 cm. A low whisking velocity (10 deg/sec) minimized inertial effects and maximized the resolution of contact angle detection. This same procedure was then done with the whisker follicles rotated 90˚ to calibrate in the vertical plane (necessary to sense whisker movements out of the plane of primary motion).

To gather experimental data, the sculpted head was fixed at the center of a cylindrical coordinate system (r, θ, z) while the array whisked at several different positions. Note that θ of this general coordinate system is not the same as the angle θ

through which the whisker deflects. The array was positioned at regular intervals of height z and angle θ. The choice of r was necessarily dictated by the requirement that the whiskers make contact with all regions of the left side of the head (Table S1).

z (cm)	θ (degrees)	r (cm)
0.000 – 2.000, 0.125 cm increments	0 – 60˚, 10˚ increments	5.00
2.125 – 3.250, 0.125 cm increments	"	4.75
3.375 – 4.250, 0.125 cm increments	"	5.50
4.375 – 6.000, 0.125 cm increments	"	5.25

Table S1. The array was positioned in regular intervals of height z and angle θ, while distance r was manually chosen to ensure whisker contact with all regions of the face.

A single whisk was performed at each position (see video). Analog signals from each whisker base were filtered at 160 Hz, sampled at 500 Hz and then passed through a zero phase forward digital filter (period = 1/2 second). The location of each contact point was then computed relative to the array. The angular component θ was taken to be the angle at which the whisker first made contact with the object (when $\dot{M}$ crossed a threshold), and the radial d component was found using Eqn. S8.

A total of 343 whisks were performed. In cases where a whisker did not make contact, or the data analysis showed that the whisker hit on the right side of the face, the data were automatically removed. All other contact points were mirror-imaged to the right side of the head. The longer whiskers captured the broad convex features, while the shorter whiskers explored the finer concave regions. Equation S8 was also used to determine when contact occurred at a whisker tip. Tip contact always resulted in an estimate of d very close to or greater than the whisker length. In the case that estimated d was greater than the whisker length, d was automatically set equal to the length. Thus, Eqn. S8 provided the critical information that contact did indeed occur at the whisker tip and not mid-length. This would not have been possible had the sensing mechanism been, for example, a simple binary contact-switch.

Note that regions of the sculpture that are concave in the horizontal plane (for any given height) are only reachable through tip contact, which accounts for 25% of the splined surface. A total of 1036 contact points on the left side were collected, with 438

points determined through Eqn. S8 to occur at or near the tip (42% of all points). The points were converted to head-centered Cartesian coordinates to simplify splining, mirror-imaged to the right side, and plotted along with the spline to create Fig. S5.

Fluid Flow Characterization Methods

To estimate the shape of a variable fluid flow profile in two dimensions, two artificial whisker arrays were arranged in a plane. The sensing mechanism was reduced to one dimension, and each of the stainless steel whiskers were replaced with highly-flexible plastic strips (0.5 cm wide by 11 cm long) to increase the surface area exposed to the flow and maximize bending. Each sensor was calibrated over a range of deflections to account for any nonlinear sensing properties. A compressed air source was centered at two distances (15 cm and 40 cm) in front of the array, and data were averaged over five seconds for each whisker. The true value of the air speed was determined by placing a Pitot tube with an attached manometer at the height of each whisker. Square root of moment (moment being proportional to distributed load) was calibrated to air speed to characterize the flow, consistent with the Bernoulli equation for incompressible flow. Ten trials were taken for both the experimental (whisker) and control (Pitot tube) data.

It is important to note that this technique does not give information about the load as a function of position along the whisker length. Instead, each whisker in the array provides a single estimate of flow velocity at a given height by integrating the moment caused by the distributed load over its length. Because the eight whiskers are at different heights, the flow profile can be characterized in the z-direction. Using whiskers of different lengths and in different array configurations could allow three-dimensional characterization of the flow pattern.

References

1. Kaneko, M., Kanayama, N. & Tsuji, T. *IEEE T. Robotic. Autom.* **14**, 278-291 (1998).
2. Clements, T. N. & Rahn, C. D. *IEEE T. Robotic.* **22**, 844-848 (2006).
3. Young, W. C. & Budynas R. G. *Roark's Formula for Stress and Strain (7th Edition)* (McGraw-Hill, New York City, New York, 2002).
4. Ueno, N., Svinin, M. M. & Kaneko, M. IEEE-ASME *T. Mech.* **3**, 254-264 (1998).
5. Szwed, M. et al. *J. Neurophysiol.* **95**, 791-802 (2006).
6. Neimark, M. A., Andermann, M. L., Hopfield, J. J. & Moore, C. I. *J. Neurosci*. **23**, 6499-6509 (2003).
7. Moore, C. I. *J. Neurophysiol*. **91**, 2390-2399 (2004).
8. Hartmann, M. J., Johnson, N. J., Towal, R. B. & Assad, C. *J. Neurosci.* **23**, 6510-6519 (2003).

Supplementary Figures

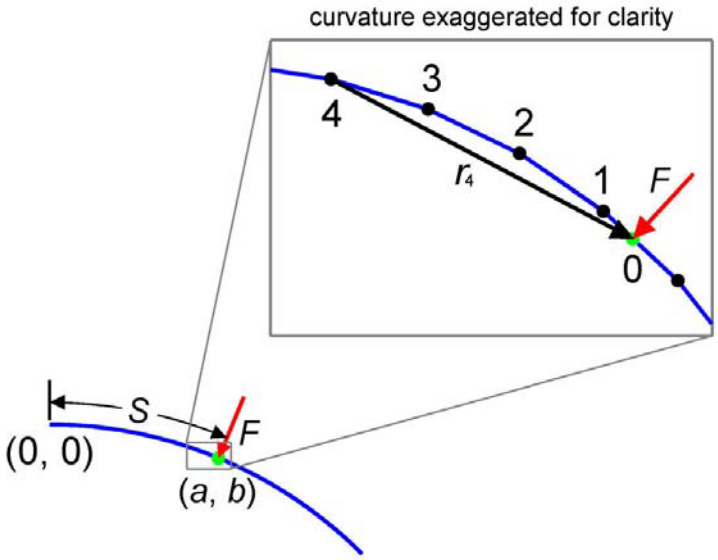

Figure S1. The shape of an inherently-curved beam deflecting due to a force *F* acting at arc length *S* from the base can be found through repeated application of Eqn. S10, starting at *S* and moving node-by-node towards the base.

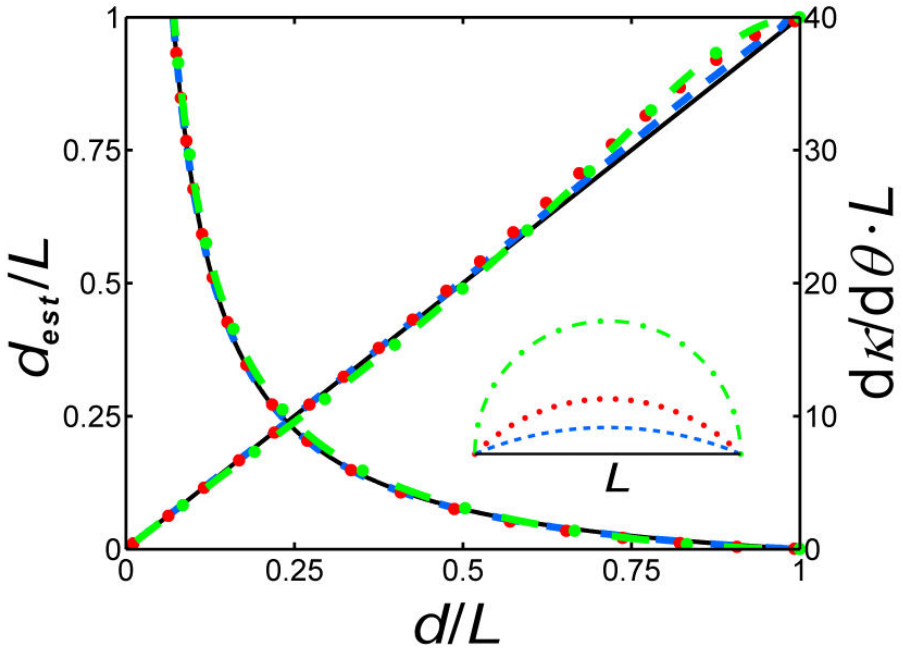

Figure S2. (left axis) Estimated contact distance from Eqn. S5 versus the actual radial distance of the point object as a numerically modeled beam (whisker) deflects into it at different distances. (right axis) Rate of curvature change (proportional to moment) at the beam base versus the actual radial distance of the peg. Black lines are analytical relationships for a straight beam. These numerical simulations confirm that whisker curvature has negligible impact on the accuracy of Eqn. S5. The blue dashed beam has a normalized curvature of $\pi/4$ (a curvature typical for rat whiskers), the red dotted beam $\pi/2$ (high for rat whiskers), and the green dash-dotted beam π (much greater than rat whiskers).

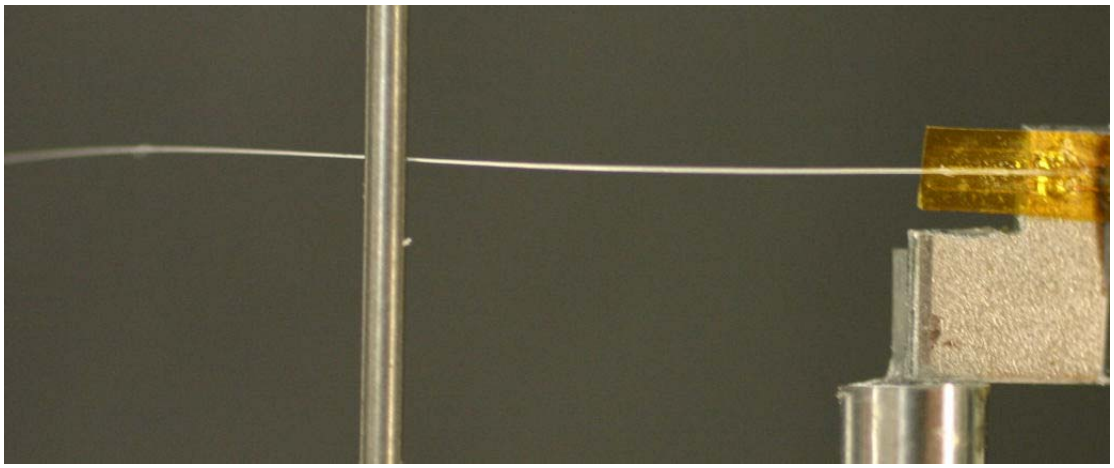

Figure S3. A rat whisker, glued to a strain gage, is smoothly rotated against a peg at varying radial distances.

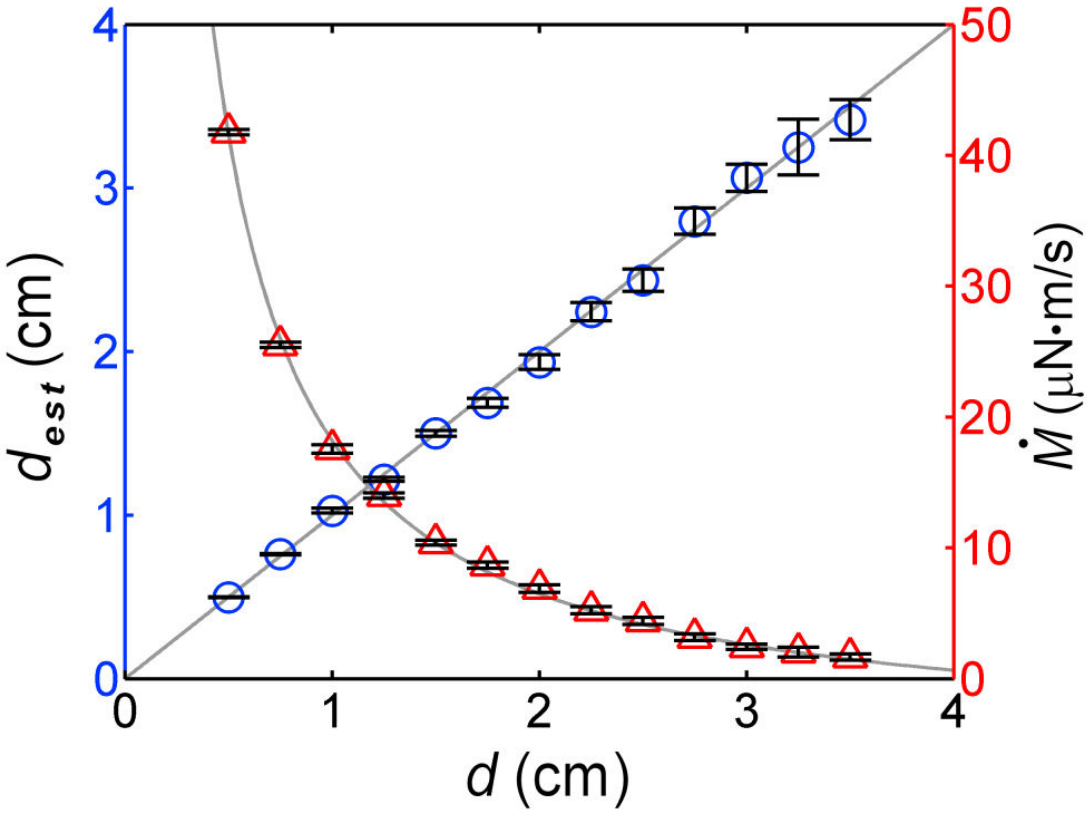

Figure S4. (blue circles) Estimated contact distance from Eqn. S5 versus the actual radial distance of the peg as a rat whisker rotates against a peg at different distances. (red triangles) Measured $\dot{M}$ versus the actual radial distance of the peg. Grey lines are analytical relationships.

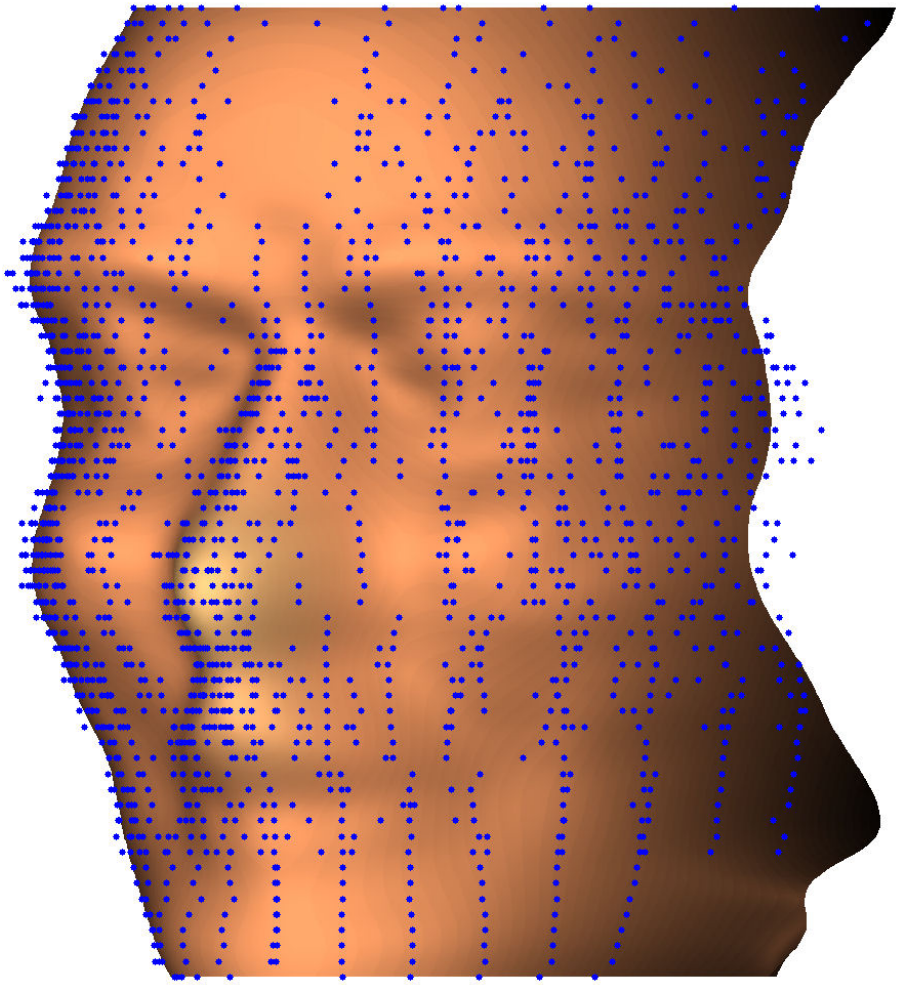

Figure S5. The complete splined surface shown in Fig. 1c, including contact points.